Oriented phosphorescent emitters boost OLED efficiency

Michael Flämmich [a], Jörg Frischeisen [b], Daniel S. Setz [c], Dirk Michaelis [a], Benjamin C. Krummacher [c], Tobias D. Schmidt [b], Wolfgang Brütting [b], Norbert Danz [a,*]

[a] Fraunhofer Institute for Applied Optics and Precision Engineering (IOF), Albert-Einstein-Str. 7, 07745 Jena, Germany
[b] Institute of Physics, Experimental Physics IV, University of Augsburg, Universitätsstr. 1, 86135 Augsburg, Germany
[c] OSRAM Opto Semiconductors, OLED-Lighting, Leibnizstr. 4, 93055 Regensburg, Germany

A B S T R A C T

The orientation distribution of the emissive sites in a phosphorescent Organic LED has been measured utilizing two independent optical methods. In contradiction to common expectations we find a clearly non-isotropic, predominantly parallel emitter orientation in the well-known triplet emitting guest–host system of $Ir(MDQ)_2(acac)$ blended in an α-NPD matrix. This result emphasizes the necessity of more sophisticated assumptions on active emitter properties in quantitative optical OLED analysis, and demonstrates a highly promising approach for OLED efficiency optimization.

Keywords:
Organic light-emitting diode
In situ characterization
Emitter orientation
Phosphorescent emitter
Photoluminescence

1. Introduction

Organic light-emitting diodes (OLEDs) [1] gain increasing interest as area light sources for general illumination [2], where energy conversion efficiency is the parameter to be improved primarily in order to tackle established lighting schemes [3]. From the electroluminescent material point of view, the advancement from singlet emitting polymeric [4] towards triplet harvesting small molecular materials [5] is commonly believed to push the internal quantum efficiency from 25% up to 100% due to charge carrier spin statistics. However, the small molecular size and the thermal evaporation process are suspected to cause an isotropic orientation distribution of the emissive sites, thus seriously limiting the optical outcoupling efficiency and overall device performance [6,7]. Additional organic electro optic devices [8] such as amplifiers [9,10] or single photon sources [11] might further exploit the emission of efficient emitters as discussed in this study.

The efficiency of OLEDs is well described by the external quantum efficiency (*EQE*) giving the number of emitted photons per injected charges [12]:

$$EQE = \gamma \cdot \eta_{S/T} \cdot q_{eff} \cdot \eta_{out}. \quad (1)$$

The *EQE* is determined by four terms. First, the charge balance factor γ accounts for the probability of charge carrier recombination and subsequent exciton formation. According to spin statistics, excited singlet as well as triplet states are generated [13]. The second term, the singlet–triplet-factor $\eta_{S/T}$, distinguishes between the two material classes of fluorescent and phosphorescent emitters. Polymeric emissive materials are usually fluorescent and singlet excited states are allowed to decay radiatively only, yielding $\eta_{S/T} = 0.25 << 1$. Small molecular emitters can utilize heavy metal ions and the resultant strong spin-orbit-coupling enables for triplet emission as well ($\eta_{S/T} = 1$), fundamentally promising higher efficiencies [5]. The third factor regards the limited internal luminescence quantum efficiency q of the excited state and the fact that the q-value becomes system dependent in any thin film stack due to coupling of the emitter to photonic modes of

* Corresponding author.
E-mail address: norbert.danz@iof.fraunhofer.de (N. Danz).

the cavity ($q \rightarrow q_{eff}$). Finally, only a fraction of the internally generated photons can leave the structure, as described by the outcoupling factor η_{out}.

The emissive process is considered as a dipole transition with the transition dipole moment having a certain orientation ϑ with respect to the normal of the surrounding layered system [7]. The emission of any arbitrarily oriented emitter can be decomposed into contributions of three orthogonal dipoles (||TE, ||TM, ⊥TM), as illustrated in Fig. 1a. These orthogonal dipoles are specified according to their orientation with respect to the interfaces of the layered system (parallel "||" with $\vartheta = \pi/2$, perpendicular "⊥" with $\vartheta = 0$) and the corresponding polarization of the emitted radiation (transverse-electric "TE", transverse-magnetic "TM"). Note that q_{eff} and η_{out} severely depend on the emitter position within the active layer as well as on the emitter orientation [14]. The OLED emission originates from an ensemble of emissive sites with an angular distribution $g(\vartheta)$ of their transition dipole moments. Then, only the relative contributions of parallel and perpendicular dipoles $p_{||}$:$p_{\perp}$ according to the integral quantities

$$p_{||} = \int_0^{\pi/2} g(\vartheta) \cdot \sin^2(\vartheta) \cdot \sin(\vartheta) d\vartheta \tag{2}$$

$$p_{\perp} = \int_0^{\pi/2} g(\vartheta) \cdot \cos^2(\vartheta) \cdot \sin(\vartheta) d\vartheta \tag{3}$$

enter the calculation [7] and will be determined experimentally in this paper.

In order to optimize the efficiency of OLEDs, the material specific electrical (γ) and optical ($\eta_{S/T}$ and q) properties as well as the layered system specific parameters (q_{eff} and η_{out}) need to be maximized. In state-of-the-art OLEDs the recombination zone is confined within a narrow layer by applying appropriate blocking materials and thus, recombination of all charge carriers is achieved ($\gamma = 1$) [15]. Utilizing phosphorescent emissive materials allows for both, singlet and triplet excitons, to decay radiatively into the ground state, yielding $\eta_{S/T} = 1$ [5]. Furthermore, emitter systems with short triplet-lifetimes and with reduced phonon mediated non-radiative relaxation processes promise the possibility of $q = 1$ [16]. However, the energy of an excited emitter can be radiated into different optical channels and only a small part of the light is finally emitted to the outside medium air, thus fundamentally limiting η_{out}. Optimizing an OLED stack enhances the emission of dipoles lying parallel to the plane of the OLED layers as this global optimum allows for extracting most power into air. Unfortunately, this optimized stack architecture tends to trap almost all light generated by perpendicularly oriented dipoles inside the layered system or the substrate glass, since perpendicular emitters undergo opposite interference conditions compared to the parallel ones [7,14]. As a result, analyzing and optimizing OLED systems require the knowledge of the emitter orientation distribution, that is generally assumed to be predominantly parallel for polymers and perfectly isotropic (a superposition of parallel and perpendicular dipoles with a ratio of $p_{||}$:$p_{\perp}$ = 2:1) for

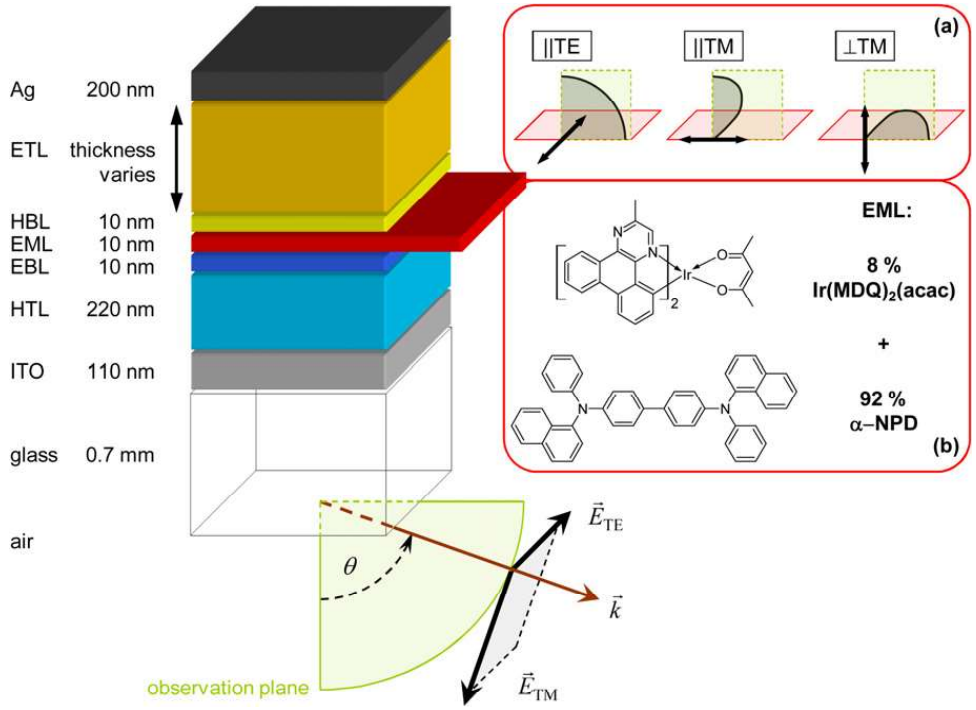

Fig. 1. Sketch of the thin film stack consisting of indium-tin oxide (ITO) as transparent anode on a glass substrate, covered by a thermally evaporated stack of hole transport (HTL), electron blocking (EBL), emitting (EML), hole blocking (HBL), and electron transport layer (ETL), contacted by a silver (Ag) cathode. The EML is prepared by co-evaporating the α-NPD matrix material with 8 wt.% of the red emitting phosphorescent dye $Ir(MDQ)_2(acac)$ as indicated in the inset. (b). An OLED series with varying ETL thicknesses from about 40 nm up to almost 400 nm has been analyzed. For angular resolved experiments, emission pattern in air has been scanned in one dimension (angle θ). The observation direction k and the orientations of the two perpendicular electric field polarization components TE and TM are drawn for convenience. The inset (a) illustrates the three basic dipoles and corresponding emission patterns assuming an infinite emitting medium. (For interpretation of the references to color in this figure legend, the reader is referred to the web version of this article.)

small molecule guest–host systems [6,7,17–23]. The simple fact that the optical outcoupling efficiency for exclusively parallel oriented emitters is about 50% larger than for emitters with isotropic orientation [6,7], suggests a highly promising OLED optimization approach.

2. Material and methods

In this paper the emitter orientation of the well-known red triplet-emitting material Iridium(III)bis(2-methyldibenzo-[f,h]quinoxaline)(acetylacetonate) [Ir(MDQ)$_2$(acac), 8 wt.%] in a *N*,*N*′-bis(naphthalen-1-yl)-*N*,*N*′-bis(phenyl)-benzidine [α-NPD] matrix is studied. The chemical structures of Ir(MDQ)$_2$(acac) and α-NPD as well as the architecture of the OLED stack are shown in Fig. 1.

2.1. OLED fabrication

OLED samples, comprising several individually addressable circular pixels of 4 mm^2 area, have been prepared by thermal evaporation of organic materials onto commercial ITO coated substrates. The layered structure (Fig. 1) was fabricated using standard evaporation techniques at a base pressure of 10^{-7} mbar and an evaporation rate of 0.05 nm/s. Doped ETL and HTL were used in order to improve electron and hole transport, respectively, introducing the dopant by co-evaporation. This technique was also used for incorporating red emitters into the EML matrix. After cathode evaporation all devices were encapsulated with a glass lid containing a getter. Analogous structures, but without getter and without cathode, have been prepared for photoluminescence experiments.

2.2. Electroluminescence (EL) emission pattern measurement

In order to access the optical far-field of the OLED, polarized angular radiation patterns have been recorded utilizing a rotational stage (CR1/M-Z7E, Thorlabs) where the OLED was mounted, and an optical detection system consisting of a wire grid linear polarizer (NT47-101, Edmund Optics) with attached achromatic waveplate (AQWP05M-630, Thorlabs), combined with a fiber coupled calibrated spectrometer (SD2000, Ocean Optics). The resulting experimental intensity data $I(\theta,\lambda)$ possess a wavelength resolution of $\Delta\lambda < 5$ nm and an angular resolution of $\Delta\theta < 0.5°$, as well as an intensity uncertainty below 2%. The OLED was driven at a current density of $j = 50$ mA/cm^2 using a constant current source (GS610, Yokogawa). Radiation patterns recorded at $j = 1$ mA/cm^2 and $j = 100$ mA/cm^2 show identical relative characteristics.

2.3. Photoluminescence (PL) radiation pattern measurement

An OLED stack without cathode and comprising 31 nm and 65 nm thick HTL and ETL layers, respectively, has been encapsulated without getter in order to enable for optically excited luminescence experiments using an almost linearly polarized continuous wave laser ($\lambda = 375$ nm). Polarized emission patterns inside the substrate have been measured by mounting the sample with an immersion coupled fused silica half cylinder on a computer controlled rotational stage. The angular dependent PL spectrum was measured with a calibrated fiber optical spectrometer and a polarizer to distinguish between TE and TM polarized emission. The measured cross sections are normalized to the values at small angles because the emission in this range occurs exclusively from parallel dipoles. Emission patterns have been shown to be independent of both, the incident angle and the polarization of the illuminating laser beam.

2.4. Radiation pattern analysis

Prior to any analysis, the wavelength-dependent, complex dispersion data ($n + i\kappa$) of all materials involved have been measured utilizing dispersion-model-free reflection–transmission-spectroscopy, a method published previously [24]. Subsequent spectral reflectivity analysis enables for exact determination of layer thicknesses. Device emission has been simulated by means of a self-developed software tool, based upon the theory of Chance, Prock, and Silbey [25–27]. By analyzing TE polarized emission following approaches presented previously [7,14], we determined the emitter's internal EL spectrum to be identical to the PL spectrum and the emission zone to be constant.

3. Results

Varying the distance between the emissive sites and the cathode by adjusting the electron transport layer (ETL) thickness imposes the most pronounced effects onto the optical device properties because of interference effects arising due to the reflection at the mirror like metal cathode. As previously demonstrated [7,14], the presence of perpendicularly oriented emitters can be visualized by adapting the ETL thickness. For the system under study, a 160 nm thick ETL induces destructive interference for emitters aligned parallel to the layers, while enhancing the emission of perpendicularly oriented emitters into the air half space, thus being a particularly sensitive probe for studying the presence of perpendicular dipoles. Fig. 2a shows the experimentally observed radiation pattern for TM polarized emission. Knowing the optical constants and layer thicknesses of all materials, the radiation pattern $I(\theta,\lambda)$ of the device is calculated according to classical theory [25], where further details can be found in previous publications [14,21,26,27]. Obviously, the experimental emission pattern is well described assuming a ratio of $p_{||}:p_{\perp} = 2:(0.63 \pm 0.07)$ for parallel vs. perpendicularly oriented emitters. Thus, the amount of perpendicularly oriented active sites is significantly lower compared to the common isotropic assumption ($p_{||}:p_{\perp} = 2:1$). Note that this result is obtained in an operating OLED differing from an optimized stack only in the increased ETL thickness.

In order to prove this surprising result, the emitter orientation has been determined independently using optically excited luminescence from an essentially identical stack without the metal cathode, following the approach presented in Ref. [6]. Again, the quantitative analysis in Fig. 3 yields a fraction of $p_{||}:p_{\perp} = 2:(0.67 \pm 0.05)$ for parallel vs. perpendicular emitters well within the confidence

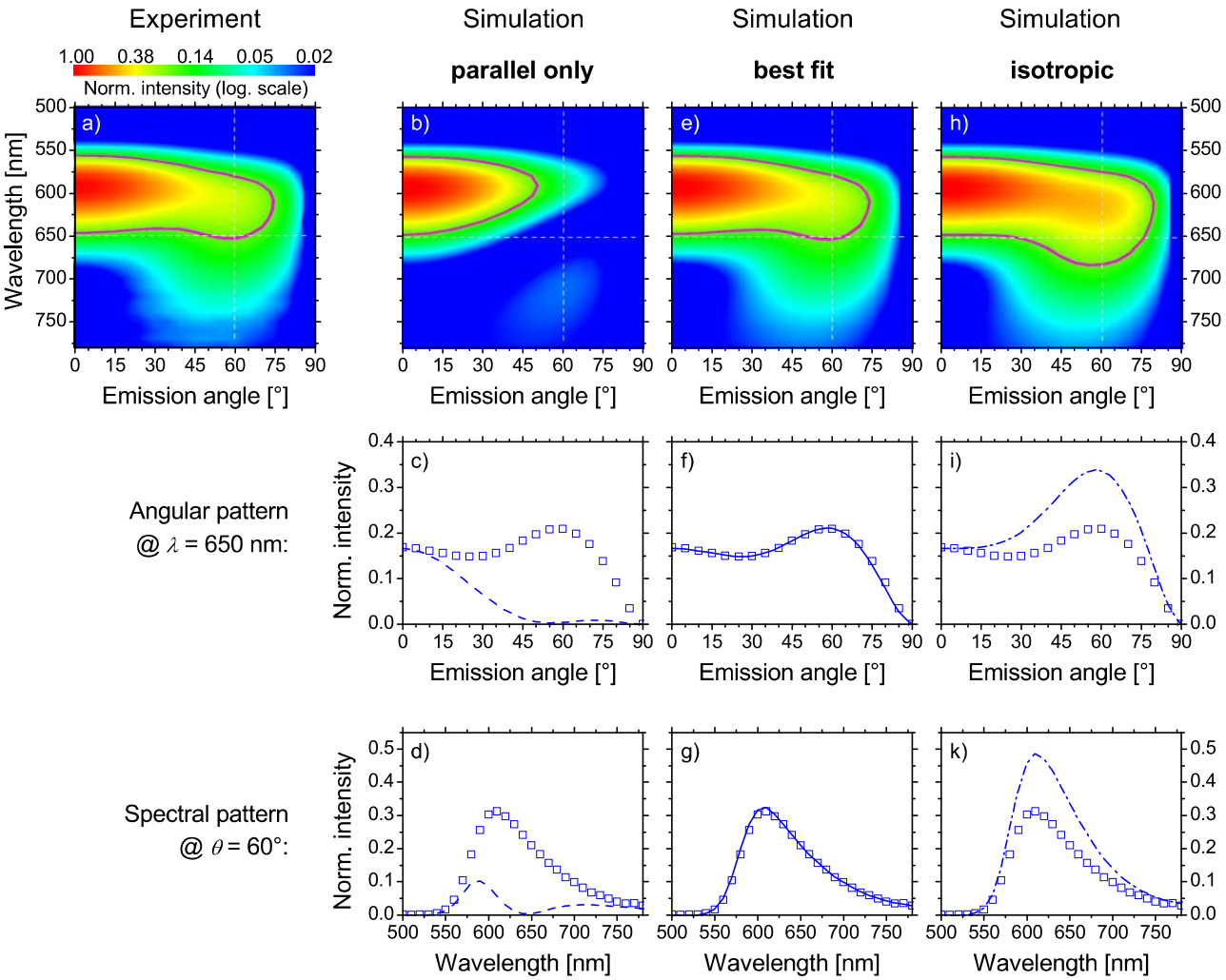

Fig. 2. Experimental and theoretical results obtained for the TM-polarized, spectral and angular resolved emission pattern $I(\theta,\lambda)$ in air of the adapted OLED comprising 160 nm ETL thickness. False color plots containing the entire spectral and angular pattern (top row; a, b, e, h) exhibit a logarithmic intensity scale to better visualize low intensity data. The value 0.2 is accentuated by a magenta line, the cross sections at angle $\theta = 60°$ and wavelength $\lambda = 650$ nm are indicated by white dashed lines. Cross section data for one fixed wavelength ($\lambda = 650$ nm; middle row; c, f, i) and one fixed angle ($\theta = 60°$; bottom row; d, g, k) are plotted with experimental results (squares) as well as the theoretical predictions (lines). Simulation results for three different emitter orientations are shown: An emitter alignment strictly parallel to the interfaces is assumed for the left "parallel" column (b, c, d); and an isotropic distribution for the right "isotropic" column (h, i, k). These two assumptions fail to yield a match to the experimental data, resulting in a "best fit" (middle column; e, f, g) assuming a fraction of 2:(0.63 ± 0.07) for parallel and perpendicular emitter contributions.

interval of the result in electrical operation, and clearly demonstrating a significant difference to the commonly assumed isotropic case.

So far, the discussion is based on a single device comprising the adapted ETL thickness of 160 nm. Additionally, quantitative radiation pattern analysis as well as emission lifetime measurements have been performed with a series of similar devices with varying ETL thickness in the 40–400 nm range (results not shown). The relative amount of perpendicular emitters could be confirmed with a device comprising a 333 nm thick ETL layer that is the second optimum for coupling of perpendicular emitters into air. Thus, the preferred parallel orientation is valid for all reasonable emitter–cathode distances, including devices which are optimized for maximum efficiency. Furthermore, no effect of pump current density on the determined orientation distribution was apparent up to 100 mA/cm^2 current density. Additionally, the internal luminescence quantum efficiency extrapolated to zero current was measured to be $q_0 = (74 \pm 4)\%$ utilizing previously published methods [22,23]. In result, we conclude that this particular emissive system is precisely described by quantitative optical simulation.

4. Discussion

The orientation distribution of Ir(MDQ)$_2$(acac) in α-NPD has been determined by two different optical methods with and without electrical excitation, both yielding identical results. The presence of non-isotropically distributed emitter ensembles in this phosphorescent guest–host system is concluded. We attribute this truly surprising result to the morphology of the α-NPD matrix blended with

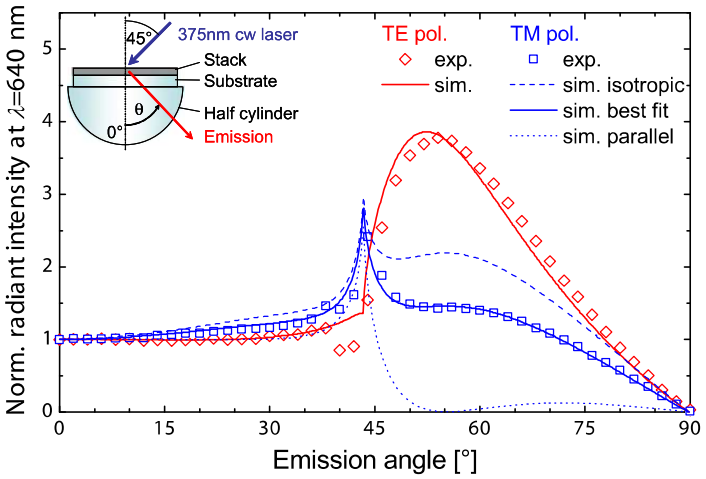

Fig. 3. Angular and polarization resolved photoluminescence emission pattern $I(\theta,640\ \text{nm})$ obtained by optical excitation at 375 nm and detection at 640 nm wavelength. An OLED stack according to Fig. 1 with HTL thickness of 31 nm and ETL thickness of 65 nm, but without the Ag cathode was used. The experimental geometry is illustrated in the inset. Data are normalized to perpendicular emission ($\theta = 0°$). Obviously, TM polarized emission is overestimated when assuming an isotropic emitter ensemble. The fit reveals a relative contribution of 2:(0.67 ± 0.05) parallel vs. perpendicular emitters.

the $Ir(MDQ)_2(acac)$ chromophore. The interaction of the asymmetric molecules during co-evaporation and the resulting predominantly parallel orientation of the dipole transition moments are not fully understood yet. We consider additional investigations potentially utilizing more sophisticated spectroscopic techniques in order to understand and to further exploit this effect.

It is worth to note that a slight birefringence of the α-NPD matrix has been observed [28] previously. Taking this effect into account yields an even more pronounced parallel emitter contribution but still within the confidence limits given.

The emitter orientation distribution obtained for the investigated small-molecular OLED emitter system reveals: the active sites in phosphorescent small molecule guest–host systems are not necessarily distributed isotropically. While the common assumption of isotropy yields a $p_{||}:p_{\perp} = 2:1$ ratio of parallel vs. perpendicularly aligned emitters, our result corresponds to a ratio of $p_{||}:p_{\perp} = 2:0.63$, i.e., a predominantly parallel orientation. Consequently, one generally accepted argument applied to discussions of triplet emitting OLED devices must be revised. Beyond doubt, there are triplet emitters with isotropic orientation, but this attribute cannot be assumed generally. By contrast, emitter orientation based optimization of OLED devices seems to be within reach, since parallel emitters preferably emit into air and, therefore, reduce the effect of surface plasmon polariton excitation at the cathode as optical loss channel. This optimization potential is illustrated by the calculations shown in Fig. 4. Assuming an optimized stack with the emitter properties obtained in this work yields 22.5% *EQE* (green curve in Fig. 4). A further emitter based optimization towards high quantum efficiency ($q = 0.95$) and an improved, predominantly parallel emitter orientation (with a ratio of $p_{||}:p_{\perp} = 2:0.14$ according to a realistic angular distribution with ±22° total width) could boost this efficiency by a factor of 1.5 to reach *EQE* = 35% (red curve in Fig. 4). Note that these efficiency values are given for the planar OLED system according to

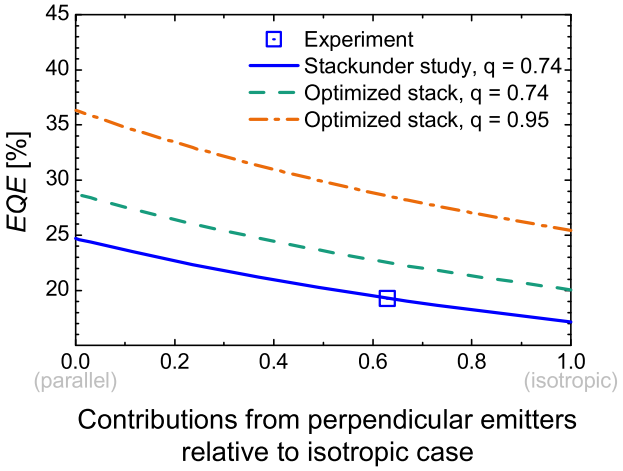

Fig. 4. OLED external quantum efficiencies vs. the relative amount x of perpendicular emitters as given in the text ($p_{||}:p_{\perp} = 2:x$). The square indicates the best value reached within this study at an ETL thickness of 250 nm. Plotting *EQE*-values simulated for this system with different amounts of perpendicular emitters yields the blue curve. Optimizing the OLED stack by varying ETL (~250 nm), HTL (~90 nm), and ITO (~90 nm) thicknesses yields the green curve with potential device efficiencies of 20–30%. Extending the simulation towards nearly ideal emitters ($q = 0.95$, red curve) provides planar devices with the highest possible efficiencies, potentially exceeding 30% *EQE*. (For interpretation of the references to color in this figure legend, the reader is referred to the web version of this article.)

Fig. 1, avoiding more or less expensive internal or external outcoupling structures.

Interestingly, *EQE*-values in excess of 30% – definitely impossible with isotropic emitters (see Fig. 4) – have been reported recently [29], but without giving a sound explanation for this unexpected high number. Our results clearly demonstrate that an *EQE*-value in this range is feasible without any outcoupling enhancement structures by using phosphorescent emitters with their transition dipole moments being preferentially oriented in the substrate plane. This opens up novel approaches for OLED efficiency improvement by using smart emissive materials with

advantageous molecular orientation. Materials design, the influence of the matrix material, and the substrate as well as film deposition conditions are just a few parameters that need to be studied further to exploit the huge potential of the dipole emitter orientation in OLEDs.

Acknowledgments

The authors thank the German Federal Ministry of Education and Research (BMBF) for funding part of this work under contract FKZ 13N10474 (TOPAS 2012). M.F. is indebted to S. Roth and T. Kümpfel for experimental assistance at Fraunhofer IOF Jena.

References

[1] C.W. Tang, S.A. VanSlyke, Organic electroluminescent diodes, Applied Physics Letters 51 (1987) 913–915.
[2] B. D'Andrade, White phosphorescent LEDs offer efficient answer, Nature Photonics 1 (2007) 33–34.
[3] S. Reineke, F. Lindner, G. Schwartz, N. Seidler, K. Walzer, B. Lüssem, K. Leo, White organic light-emitting diodes with fluorescent tube efficiency, Nature 459 (2009) 234–239.
[4] J.H. Burroughes, D.D.C. Bradley, A.R. Brown, R.N. Marks, K. Mackay, R.H. Friend, P.L. Burns, A.B. Holmes, Light-emitting diodes based on conjugated polymers, Nature 347 (1990) 539–541.
[5] M.A. Baldo, D.F. O'Brien, Y. You, A. Shoustikov, S. Sibley, M.E. Thompson, S.R. Forrest, Highly efficient phosphorescent emission from organic electroluminescent devices, Nature 395 (1998) 151–154.
[6] J. Frischeisen, D. Yokoyama, C. Adachi, W. Brütting, Determination of molecular dipole orientation in doped fluorescent organic thin films by photoluminescence measurements, Applied Physics Letters 96 (2010) 073302.
[7] M. Flämmich, M.C. Gather, N. Danz, D. Michaelis, A.H. Bräuer, K. Meerholz, A. Tünnermann, Orientation of emissive dipoles in OLEDs: quantitative in situ analysis, Organic Electronics 11 (2010) 1039–1046.
[8] J. Clark, G. Lanzani, Organic photonic for communications, Nature Photonics 4 (2010) 438–446.
[9] M.C. Gather, K. Meerholz, N. Danz, K. Leosson, Net optical gain in a plasmonic waveguide embedded in a fluorescent polymer, Nature Photonics 4 (2010) 457–461.
[10] I. De Leon, P. Berini, Amplification of long-range surface plasmons by a dipolar gain medium, Nature Photonics 4 (2010) 382–387.
[11] K.G. Lee, X.W. Chen, H. Eghlidi, P. Kukura, R. Letow, A. Renn, V. Sandoghdar, S. Götzinger, A planar dielectric antenna for directional single-photon emission and near-unity collection efficiency, Nature Photonics 5 (2011) 166–169.
[12] R.H. Friend, R.W. Gymer, A.B. Holmes, J.H. Burroughes, R.N. Marks, C. Taliani, D.D.C. Bradley, D.A. Dos Santos, J.L. Bredas, M. Lögdlund, W.R. Salaneck, Electroluminescence in conjugated polymers, Nature 397 (1999) 121–128.
[13] M.A. Baldo, D.F. ÓBrien, M.E. Thompson, S.R. Forrest, Excitonic singlet–triplet ratio in a semiconducting organic thin film, Physical Review B 60 (1999) 14422–14428.
[14] M. Flämmich, D. Michaelis, N. Danz, Accessing OLED emitter properties by radiation pattern analyses, Organic Electronics 11 (12) (2011) 83–91.
[15] M. Pfeiffer, K. Leo, X. Zhou, J.S. Huang, M. Hofmann, A. Werner, J. Blochwitz-Nimoth, Doped organic semiconductors: physics and application in light emitting diodes, Organic Electronics 4 (2003) 89–103.
[16] Yersin, H, Highly Efficient OLEDs with Phosphorescent Materials (Wiley-VCH Verlag GmbH & Co. KGaA, Weinheim, 2008).
[17] J.A.E. Wasey, A. Safonov, I.D.W. Samuel, W.L. Barnes, Effects of dipole orientation and birefringence on the optical emission from thin films, Optics Communication 183 (2000) 109–121.
[18] J.-S. Kim, P.K.H. Ho, N.C. Greenham, R.H. Friend, Electroluminescence emission pattern of organic light-emitting diodes: implications for device efficiency calculations, Journal of Applied Physics 88 (2000) 1073–1081.
[19] L.H. Smith, J.A.E. Wasey, W.L. Barnes, Light outcoupling efficiency of top emitting organic light-emitting diodes, Applied Physics Letters 84 (2004) 2986–2988.
[20] J.M. Ziebarth, M.D. McGehee, A theoretical and experimental investigation of light extraction from polymer light-emitting diodes, Journal of Applied Physics 97 (2005) 064502.
[21] S. Nowy, B.C. Krummacher, J. Frischeisen, N.A. Reinke, W. Brütting, Light extraction and optical loss mechanisms in organic light-emitting diodes: influence of the emitter quantum efficiency, Journal of Applied Physics 104 (2008) 123109.
[22] B.C. Krummacher, S. Nowy, J. Frischeisen, M. Klein, W. Brütting, Efficiency analysis of organic light-emitting diodes based on optical simulation, Organic Electronics 10 (2009) 478–485.
[23] M. Flämmich, M.C. Gather, N. Danz, D. Michaelis, K. Meerholz, In situ measurement of the internal luminescence quantum efficiency in organic light-emitting diodes, Applied Physics Letters 95 (2009) 263306.
[24] M. Flämmich, N. Danz, D. Michaelis, A. Bräuer, M.C. Gather, J.H.-W.M. Kremer, K. Meerholz, Dispersion-model-free determination of optical constants: application to materials for organic thin film devices, Applied Optics 48 (2009) 1507–1513.
[25] R.R. Chance, A. Prock, R. Silbey, Molecular fluorescence and energy transfer near interfaces, Advances in Chemical Physics 37 (1978) 1–65.
[26] N. Danz, R. Waldhäusl, A. Bräuer, R. Kowarschik, Dipole lifetime in stratified media, Journal of the Optical Society of America B: Optical Physics 19 (2002) 412–419.
[27] N. Danz, J. Heber, A. Bräuer, R. Kowarschik, Fluorescence lifetimes of molecular ensembles near interfaces, Physical Review A 66 (2002) 063809.
[28] D. Yokoyama, A. Sakaguchi, M. Suzuki, C. Adachi, Horizontal molecular orientation in vacuum-deposited organic amorphous films of hole and electron transport materials, Applied Physics Letters 93 (2008) 173302.
[29] P. A. Levermore, V. Adamovich, K. Rajan, W. Yeager, C. Lin, S. Xia, G. S. Kottas, M. S. Weaver, R. Kwong, R. Ma, J. J. Brown, M. Hack, Highly efficient phosphorescent OLED lighting panels for solid-state lighting. presentation at 48th Society for Information Display Symposium (Seattle, May 27, 2010); Hack, M. Phosphorescent OLED Technology for Energy Efficient Solid State Lighting. Presentation at 6th Global Plastic Electronics Conference & Exhibition (Dresden, October 21, 2010).